Frequency Control of Multi-Pulse 2-micron Laser Transmitter for Atmospheric Carbon Dioxide Measurement

Mulugeta Petros
Remote Sensing Branch
NASA Langley Research Center
Hampton, USA
mulugeta.petros-1@nasa.gov

Tamer Refaat
Remote Sensing Branch
NASA Langley Research Center
Hampton, USA
tamer.f.refaat@nasa.gov

Upendra N. Singh
NASA Engineering Safety Center
NASA Langley Research Center
Hampton, USA
upendra.n.singh@nasa.gov

Charles W. Antill
Remote Sensing Branch
NASA Langley Research Center
Hampton, USA
charles.w.antill@nasa.gov

Ruben G. Remus
Flight Software Systems Branch
NASA Langley Research Center
Hampton, USA
ruben.g.remus@nasa.gov

Teh-Hwa Wong
Science Systems & Applications
NASA Langley Research Center
Hampton, USA
teh-hwa.wong@nasa.gov

Jane Lee
Science Systems & Applications
NASA Langley Research Center
Hampton, USA
jane.lee@nasa.gov

Syed Ismail
Analytical Services & Materials
NASA Langley Research Center
Hampton, USA
syed.ismail@nasa.gov

Abstract— **Laser sources with highly stabilized emission wavelength is of paramount importance for a long term atmospheric carbon dioxide (CO_2) measurement from a space platform. Integrated Path Differential Absorption (IPDA) lidar is a promising instrument for such a task. The design of a laser transmitter, with emphasis on the method used to control and select several wavelengths, is presented. This multi-pulsed, injection seeded, 2-µm transmitter uses a Ho:Tm:YLF laser crystal which has matching emission to the absorption of CO_2 in the R30 spectroscopic area. The injection seeded laser produces triple single longitudinal mode transform limited line width pulses with a total of 80 mJ at a repetition rate of 50 Hz.**

Keywords—carbon dioxide; seed laser; injection seeding IPDA; lidar; multi-pulse laser

I. INTRODUCTION

Accurate and precise measurement of the carbon dioxide (CO_2) column averaged dry air mixing ratio requires a high quality laser transmitter with very high spectral purity, low jitter and minimum offset from the desired wavelength to reduce random and systematic errors [1]. These errors are accumulated and affects the CO_2 optical depth measurements, which is the primary product of the integrated path differential absorption (IPDA) lidar. The demonstrated IPDA lidar consists of a laser transmitter operating at 50Hz producing three pulses separated by 200 µs; a wavelength control system that provides multiple wavelengths required for seeding each pulse at a different wavelength; an electronics system to synchronize and control the timing between the various sub-systems of the lidar; a cooling system to remove and manage the thermal loads in the laser and other thermally sensitive components; and a receiver system that includes a 40 cm telescope, aft optics, bore-sight, detectors and a data acquisition and processing system. The IPDA lidar technique requires multiple wavelengths to satisfy the differential measurement requirements with respect to spectroscopic signature. For generating these wavelengths, it is important that the laser transmitter has a seed laser source with extremely narrow line width. In the case of a high energy transmitter, injection seeding is required. Several methods of seeding pulsed lasers have been proposed and presented. However, for a high vibration environment such as airborne systems, the ramp and fire scheme is preferable. This seeding technique occurs within microseconds, which is much faster than any physical motion thus resulting in a system immune to vibration. However, since the pulsed laser is fired while the cavity length is changing, additional offsets and jitters are introduced. Therefore it is essential to measure the output pulse wavelength or frequency using, for example, a heterodyne detection scheme and relating it to the return signal. A careful selection of the on- and off-line frequencies around the R30 CO_2 absorption line with low temperature sensitivity and minimum H_2O interference is also important.

II. SEED LASER

A. *Distributed feedback semiconductor laser*

A custom semiconductor distributed feedback diode (DFB) laser is used as a seed source. The DFB is installed in a 14 pin butterfly package with an integrated isolator. The output is delivered with a polarization maintaining fiber. The DFB is excited using 400 mA and produces up to 15 mw at 2.05 µm. The single longitudinal mode radiation has a linewidth narrower than 200 KHz [2]. An electronic circuit is designed to drive the DFB and control the operating temperature to within 0.0001 K. The free running long and short term drifts and jitters as well as power stability of the device were characterized prior to locking to a CO_2 cell. The long term DFB output power stability measurement was conducted with more than 2.2 M samples collected during 83 minutes using a power meter (Melles Griot 13PEM001 Broadband Power/Energy Meter). Statistical analysis was obtained by observing the number of occurrence of each power level within the sampling bin. Gaussian fitting resulted in a measured power mean and standard deviation of 5.97±0.05 mW. The same procedures were applied to obtain the wavelength long term stability, through 12.5 K wavelength samples collected during 77 minutes using a wavemeter (Bristol Wavelength Meter, Model 621) and the number of occurrence was observed for 0.01 pm wavelength bins. Gaussian fitting resulted in a mean and standard deviation of 2050.9665 nm and 0.086 pm, respectively. This standard deviation translates to ±6.2 MHz wavelength jitter in an unlocked operation, given that 1 pm wavelength is equivalent to 72 MHz in the neighborhood of the 2-μm wavelength. This drives the need for more precise center line locking electronics.

B. CO_2 center line locking

A standard Pound-Drever-Hall (PDH) frequency stabilization scheme was implemented to lock the DFB wavelength to the absorption peak of the CO_2 R30 line. The optical section of the locking system consists of fiber based devices. A 200 MHz electro-optic (EO) modulator is used to generate two wavelengths offset by ±2.78 pm from the center wavelength. The modulated output was applied to a CO_2 filled absorption cell. The cell is 50 mm long and has 37 torr of pressure. The output of the cell is detected and directed into the locking electronics. The electrical signal is filtered at the modulation frequency, amplified, and mixed with the 200 MHz local oscillator signal. The phase is adjusted to compensate for the path mismatch between the two signals to produce an error signal. A servo control is used that precisely locks the DFB to the absorption peak of the CO_2 by adjusting the current and temperature of the device. To measure the wavelength jitter, the deviation of the control signal at the zero crossing is compared to the linear portion of the error slope. A million samples of this signal was taken, averaged and the mean and the standard deviation was 2050.966697 nm and 0.00913 pm. This standard deviation translates to ±657.6 kHz of wavelength jitter [4].

C. Side-line generation

The line center is used as a reference to offset wavelengths used as on and off-line. The off-line is generated by modulating the center line with an EO modulator. The modulator generates ±225.3 pm peaks. The center line and the shorter wavelength are suppressed and the longer wavelength, which is 2050.191997 nm, is selected due to lower water vapor interference. For the on-line, a range of wavelengths, spanning from the R30 center line up to 4 GHz away, which corresponds to 2051.023 nm, could be used. In order to generate these wavelengths a second DFB, with similar specifications as the first, is used. A beat note is generated by using the line center from the first laser and the output of the second laser. The beat note passes through an amplifier to achieve a 0 dB amplitude. The signal is then fed into a frequency down converter based electronics which allows tuning the laser to the desired on-line wavelength. The on- and off-line wavelengths pass through a switch and an optical amplifier before it is applied as a seed source. Therefore, the system has the capability to operate in a tunable on-line wavelength and a single off-line wavelength. The choice of the on-line wavelength is determined by the projected optical depth requirement to achieve certain measurement objectives [3]. Generally, it is desirable to keep the IPDA measured differential optical depth close to 1. Lower differential optical depth leads to poor sensitivity, assuming random error is dominated by detection noise. On the other hand, higher differential optical depth results in lower on-line return signal. Therefore, for short range measurements, the on-line wavelength can be set closer to the line center. For longer range the on-line offset can be set around 4 GHz.

Identify applicable funding agency here. If none, delete this text box.

III. Laser transmitter

A. Transmitter architecture

The active laser material of the transmitter is Holmium and Thulium doped in Yttrium Lithium fluoride (Ho:Tm:YLF). Simulations with various degrees of complexity have been conducted for a thorough description of the energy-transfer processes involved in the laser dynamics of the co-doped Tm and Ho YLF crystals. From quantum mechanical determination of crystal field parameters to derived energy set of rate equations of the lowest four manifolds of Ho and Tm are being studied and experimentally validated by several authors [5-9]. This material system has a high emission cross-section between 2050 nm and 2064 nm with the shorter wavelength well matching the absorption of the CO_2. The long upper laser level lifetime of both Tm and Ho makes this crystal attractive for its unique capability of generating a terrain of Q-switched pulses using a single pump pulse [10]. A 792 nm pump excites the Tm $^3H_6$ to $^3H_4$ which populates the Tm $^3F_4$ level as a depository for pumping Ho. The 2-μm pulse is emitted in the transition from Ho $^5I_7$ to $^5I_8$. Since the time constant of the energy transfer between the Tm $^3F_4$ and the Ho $^5I_7$ is longer than the duration of the laser emission, the energy stored in the Tm $^3F_4$ stays intact and keeps on delivering more energy to the Ho, thereby allowing multiple pulses even after Tm pumping has stopped. The Ho and Tm co-doped approach offers the advantage of overall system simplicity. Another approach is to separate the Tm and the Ho hosts, and pump the Ho with a 1.9 μm laser. The later approach has a much lower quantum defect but does not easily lend itself to multiple pulse generation. The main 2-μm transmitter requirements are shown in Table 1.

Since the 2-μm emission occurs between the Ho $^5I_7$ and $^5I_8$, (ground level) heat removal from the lower laser level is essential. Particularly if high energy operation with a combination of high repetition rate is required. A ring resonator with two crystals is considered to avoid spatial hole burning and to facilitate injection seeding. The ring resonator is formed with six mirrors, where four mirrors are used to end-pump the crystals. Pumping the two crystals from both ends reduces the heat load by distributing the 940mJ of total pump energy over four surfaces. This mitigates the high heat load posed by the unfavorable quantum defect. Tm concentration lowered to 2% from the traditionally used 6%. This reduces the absorption coefficient and allows better infiltration of pump beam in the crystal, thereby improving pump uniformity. For enhanced Q-

TABLE 1 TRANSMITTER SPECIFICATIONS FOR THE CO_2 IPDA

Laser material	Ho:Tm:YLF
Concentration Tm/Ho (%)	2-5/0.7-1
Output energy (mJ)	40/26/14 on/ on/off
On-Line Wavelength(nm)	2050.9667-2051.023
Off-Line Wavelength(nm)	20051.1919
Repetition rate (Hz)	50/50/50
Pulse separation (µs)	~250
Pulse length(ns)	25-50
Line width(MHz)	Transform limit
Beam Quality	< 2
Frequency accuracy	< 1MHz
Beam divergence (µrad)	300

switch operation, the Ho concentration has been raised to 1%. Higher Ho concentration imposes a higher threshold condition but it enables favorable storage in the $^5I_7$ manifold for better Q-switch performance [11]. For this application, a 2 mm square by 15 mm long crystal is considered, which is conductively cooled through copper mount to 10º C. Water chillers are used to maintain the copper mount temperature by dumping the heat loss. The crystal has a very low thermal conductivity of 0.015 cal/cm-sec-°C and a linear thermal expansion of 13.8 ppm and 8 ppm per °C for the a-axis and c-axis respectively in the range of 0 -100 °C. Making the crystal any smaller reduces the cooling surface area exposing it to thermal fracture. The resonator is 1m long. All the mirrors, with the exception of the output coupler, have a 2 m concave radius of curvature, coated with a high reflector for 2051 nm and are anti-reflective for the 792 nm. The reflectivity of the output coupler flat mirror is 0.55. One of the mirrors is mounted on a ring piezo-electric actuator for cavity length adjustment during the injection seeding process. The pump is composed of laser diode arrays, fiber coupled to a 0.21 numerical aperture and 0.2 mm beam diameter. The M^2 of the pump is on the order of 87 which makes it challenging to focus the beam onto a tight spot on the order of sub millimeter along the length of the laser crystal length with a single focal lens. Multiple combinations of positive and negative lenses were used to set a 540 µ-m pump beam radius in the crystal. The laser output reaches 80 mJ for three pulses. This equates to an optical to optical efficiency of 8.5% with respect to the pump beam. This shows that with a proper thermal design, the co-doped Ho:Tm system can be as efficient as the single doped system.

B. Transmitter pulse versatility

The design of the laser allows the emission of up to four seeded pulses. The energy of each pulse can be adjusted by moving the Q-switch timing along the gain profile and changing the separation of the pulses. This adds flexibility to the transmitter operation. For example, the transmitter has recently been used to measure two different species, water vapor (H_2O) and CO_2 using three pulses. Pulse 1 and pulse 2 were used as the H_2O on- and off-line, while pulse 2 and 3 were used as the CO_2 on- and off-line. In this case, the seed wavelength change occurs after every Q-switch pulse. For single species measurements, the extra pulses can be used for further calibration by transmitting two on- or two off-line pulses.

C. Injection seeding

Since the outset of the invention of lasers, researchers have devised methods to improve the wavelength stability of lasers using an optical analog of microwave-oscillators stabilization techniques [11-12]. Although there are a myriad of approaches to achieve single longitudinal mode output, for a pulsed laser, the most frequently used approach involves the use of a low power single mode laser injected and resonated into the high power oscillator cavity and lowering the cavity loss at the instant of resonance peak. The underlining concept of injection seeding depends on having a much narrower bandwidth laser to be injected near one of the axial mode frequencies of the high power oscillator and have the pulse build up from the injected seed beam rather than the noise. A detailed theoretical treatment of injection seeding is presented by Y. K. Park et al [13]. Nevetheless, this work differs from earlier work, by repeating the injection seeding multiple times in a single pump pulse and switching the seeded wavelengths between pulses to produce three or more different frequencies to satisfy the differential absorption lidar requirements. A mode matched seed laser is injected through the output coupler in the resonator after passing through a 60dB isolator and a half wave plate to adjust the polarization. Near the peak of the population inversion, the piezo-electric actuator is ramped to generate a 2 to 3 µm travel producing a single resonance for each pulse. The ramp is configured to create four resonances with a pair of ascending and descending waveforms. The rise and fall time of the ramp is set to 75 µs. The resonance peak is electronically detected and compared to a DC voltage to setup a threshold condition for firing the laser by removing the radio frequency from the 27 MHz acousto-optic Q-switch. The amplitude of the threshold can be used to fine-tune the output pulse wavelength. For best seeding, with the minimum wavelength offset from the seed frequency, the threshold should be kept close to the resonance peak. The pulses produced have transform limited linewidth with the pulse lengths ranging from 25 to 50 ns The beam quality (M^2) of the transmitter is 1.05. For seeding verification a fast temporal pulse detector was used, as shown in Fig. 1. Although the detector has the capability to resolve mode beating if the laser is not operating in a single longitudinal mode, it does not provide additional information about the wavelength offset and jitter. Therefore, an additional heterodyne detection device is installed for monitoring the wavelength jitter and offset on every shot. Fig. 2 shows the block diagram of the heterodyne detection system. To realize this measurement, the switched seed laser is split with a 90%/10% splitter, where the 90% is directed to seed the power oscillator while the 10% is divided again with the 10% for occasional monitoring of the wavelength with a wave meter and the 90% is routed to a 100 MHz acousto optics modulator (AOM) to generate a 100 MHz intermediate frequency. The output of the AOM is mixed with a sample of the temporal pulse using a 50%/50% fiber combiner and is detected with a high bandwidth detector to produce the heterodyne signature shown in Fig. 3. The Fast Fourier Transform (FFT) of this signature shows a peak at 100 MHz for

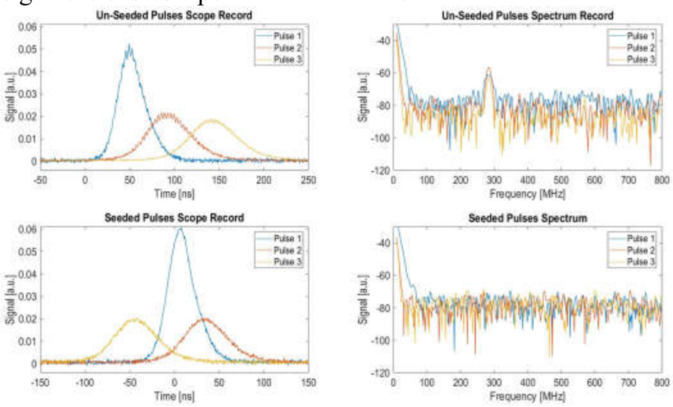

Fig. 1. Triple-pulse, 2-µm IPDA seeding verification. The plots show unseeded temporal pulses with mode beating (top left), the FFT shows a 289 MHz spectral peak corresponding to the cavity free spectral range (top right), bottom plots show clean temporal pulse with no peak in the spectrum.

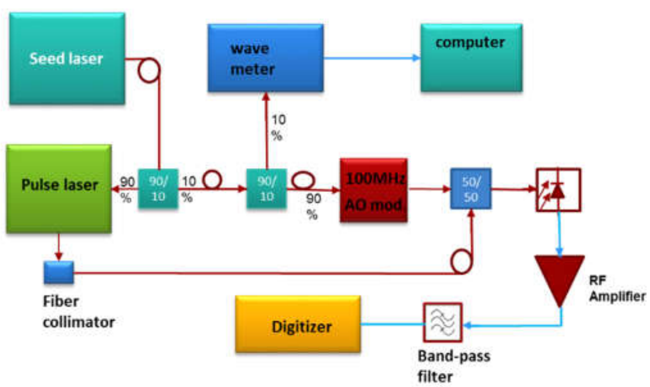

Fig. 2. Heterodyne detection block diagram in the laser transmitter.

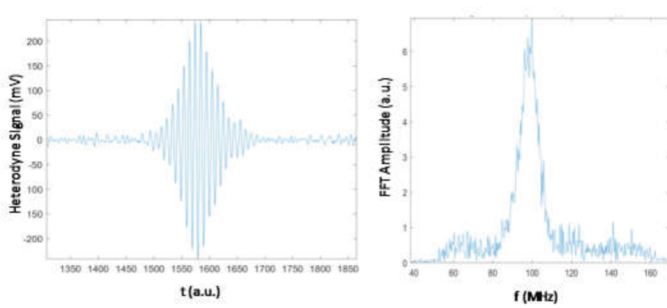

Fig. 3. Heterodyne signature (left) with corresponding FFT (right).

zero deviation from the seed laser wavelength. The full–width-half-max of the FFT represents the line width of the pulse.

IV. Conclusions

A transmitter for a novel IPDA lidar system capable of measuring multiple atmospheric species such as CO_2 and H_2O independently and simultaneously from an airborne platform was developed. The design feature considers a scheme of wavelength control system that locks the narrow line width laser to a CO_2 absorption cell for absolute wavelength control. Careful selection of the appropriate on- and off-lines is based on spectroscopic analysis. Injection seeding of multiple frequencies to produce high energy pulsed outputs, and an on-line monitoring of the wavelength is incorporated into the lidar system. All the different sub-systems have been designed, built and characterized. Airborne measurements are planned in conjunction with other CO_2 sensors such as NOAA's flask air-sampling for IPDA validation. Airborne measurements will be conducted in various environments and ground reflectivity conditions such as vegetation, snow, sand and ocean during day and night. This IPDA lidar development opens a path toward space-based active remote sensing.

References

[1] U. Singh, B. Walsh, J. Yu, M. Petros, M. Kavaya, T. Refaat, and N. Barnes, "Twenty years of Tm:Ho:YLF and LuLiF laser development for global wind and carbon dioxide active remote sensing," Opt. Mate. Express, 5(4), 827 (2015).

[2] Mahmood Bagheri, Gary D. Spiers, Clifford Frez, Siamak Forouhar, "Line width Measurement of distributed-feedback semiconductor Lasers operating near 2.05-µm," IEEE Photonics Technology Letters, 27(18) 15 (2015).

[3] U. Singh, T. RefaatT, S. Ismail, K. Davis, S. Kawa, R. Menzies, and M. Petros, "Feasibility study of a space-based high pulse energy 2 µm CO2 IPDA lidar," Applied Optics, 56(23) 6531 (2017).

[4] T. Refaat, M. Petros, C. Antill, U. Singh and J. Yu, "Wavelength locking to CO_2 absorption line-center for 2-µm pulsed IPDA lidar application," Proc. SPIE, 9879, 987904 (2016).

[5] Brian M. Walsh, Norman P.Barnes, Mulugeta Petros, Jirong Yu , Upendra N. Singh, " Spectroscopy and modeling of solid state lanthanide laser: Applicatio to triavalent TM^{3+} and Ho^{3+} in $YLiF_4$ and $LuLiF_4$ " Journal of Applied Physics 95(7)3255-3271 (2004).

[6] N. P. Barnes, E. D. Filer, C. A. Morrison, and C. J. Lee, "Ho:Tm lasers. I: Theoretical," IEEE J. Quantum Electron. 32(1), 92–103 (1996).

[7] G. Rustad and K. Stenerson, "Modeling of laser-pumped Tm and Ho lasers accounting for up conversion and ground-state depletion," IEEE J. Quantum Electron. 32**,** 1645–1656 (1996).

[8] N. P. Barnes, W. J. Rodriguez, and B. M. Walsh, "Ho:Tm:YLF laser amplifiers," J. Opt. Soc. Am. B 13**,** 2872–2882 (1996).

[9] E. D. Filer, C. A. Morrison, N. P. Barnes, and B. M. Walsh, "YLF isomorphs for Ho and Tm applications," in *Advanced Solid-State Lasers*, T. Y. Fan and B. Chai, eds., Vol. 20 of OSA Proceedings Series Optical Society of America, Washington, D.C., pp. 127–130(1994).

[10] Didier Bruneau, Stéphane Delmonte, and Jacques Pelon "Modeling of Ho,Tm:YAG and Ho,Tm:YLF 2-micron lasers and calculation of extractable enrrgies" Appl. Opt., Vol. 37(38)8406-8419(1998).

[11] Oleg A. Louchev, Yoshiharu Urata and Satoshi Wada "Numerical simulation and optimization of Q-switched 2-µm Tm:Ho:YLF laser" OPTICS EXPRESS Vol. 15, No. 7 pp. 3946 (2007).

[12] Morley S. Lipsett and Paul H. Lee, "Laser wavelength Stabilization with a Passive Interferometer," Appl. Opt., 5(5), 823 (2015).

[13] Y. K. Park, G, Guliani, Robert L. Byer "Single Axial Mode Operation of a Q-Switched Nd:YAG Oscillator by Injection Seeding," IEEE J. Quantum Electron. 20(2) 119–125 (1984).